NORTH POLAR COLOR MOSAIC OF THE MOON ACQUIRED BY LROC WAC. H. Sato[1,4], B. W. Denevi[2], B. Hapke[3], M. S. Robinson[4], H. Otake[1], [1]Japan Aerospace Exploration Agency, 3-1-1 Yoshinodai, Tyuo-ku, Sagamihara, Kanagawa, Japan (satoh.hiroyuki@jaxa.jp), [2]Johns Hopkins University Applied Physics Laboratory, Laurel, MD, [3]University of Pittsburgh, Pittsburgh, PA, [4]Arizona State University, Tempe, AZ.

Introduction: The Lunar Reconnaissance Orbiter Camera (LROC) Wide Angle Camera (WAC) has acquired ~284,000 multispectral observations over eight years of mission operations since September 2009. The significant numbers of repeated observations near the pole achieved a database that covers all the possible illumination and observation angles. Additionally, the WAC acquired a special series of forward-pitch oblique (up to 45°) observations [1] that extend the available phase angle range (to the lower values) at high latitudes (>50°N).

From this WAC observation database with the rich angle variations, we derived a 7-color (321-689 nm) mosaic of the north pole. Using the derived polar color mosaic, we examined the existence of latitudinal color trend that has been discussed by several works [e.g., 2,3].

Methodology: We derived the WAC polar color mosaic by the tile-by-tile method [4]. First, we calculated the Hapke parameters (***w***, ***b***, and ***hs***)[5] for each 30 by 30 km tile (equivalent to 1° by 1° tile at the equator). Using the derived parameters, we normalized the reflectance to the common illumination and viewing geometries (incidence ***i*** = phase ***g*** = 60°, emission ***e*** = 0°) and derived an image patch (76 by 76 pixels; ~400 m/pixel) for each tile. Each pixel consists of a median value of all the repeated observations. All the patch images are merged together into a large polar "median" mosaic; latitude from 62° to 90°N, longitude from 0° to 360°E.

Due to the systematically increasing angle ***i*** toward the pole, all the topographic reliefs (e.g., fractures and wrinkles) are emphasized. Furthermore, the footprint size of each pixel varies depending on the wavelength (UV: ~400 m, visible: ~100 m), spacecraft altitude, and pixel position within a frame (~75 m at nadir and ~100 m at edge pixels in visible bands at 50-km altitude)[6]. Therefore the accurate calculations of the ***i*** and ***e*** angles based on a high-resolution digital terrain model (DTM) are required to accurately remove the color artifacts caused by the local topographies [7]. We used the Kaguya Terrain Camera (TC) DTM (SLDEM2013; down-sampled to 60 m/pixel)[8] below 75°N and Lunar Orbiter Laser Altimeter (LOLA) DTM (30 m/pixel)[9] above 75°N. There are 1,281 images of the forward-pitch observations (~3 months of pitch observation sequences) and ~271,000 images of normal nadir observations. We used both observations, resulting in ~150±50 (UV bands) and ~500±180 (visible bands) observations per pixel (~400 m/pixel).

Results and Discussions: The north-polar Hapke parameter map (Fig. 1) shows higher single scattering albedo ***w*** on the ejecta of immature craters (e.g., Anaxagoras, Catena Sylvester, Rozhdestvenskiy K,

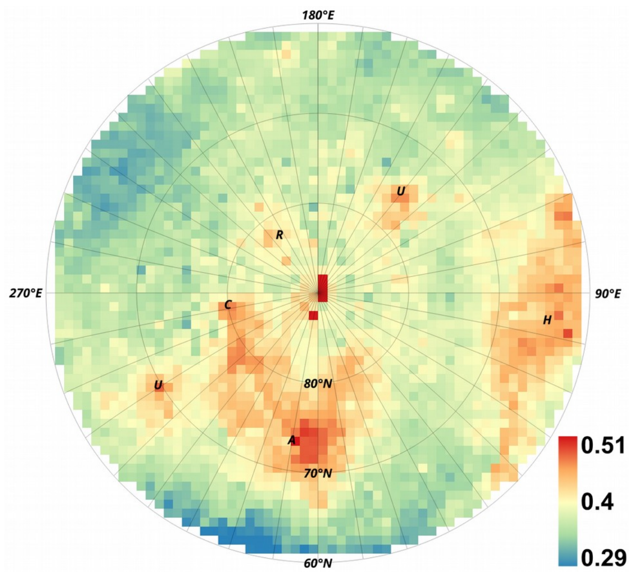

Figure 1. North polar Hapke parameter map (single scattering albedo ***w***) in 643 nm band in the Cassini projection. Characters indicate the locations of young craters (**A**: Anaxagoras, **C**: Catena Sylvester, **R**: Rozhdestvenskiy K, **H**: Hayn, and **U**: unnamed).

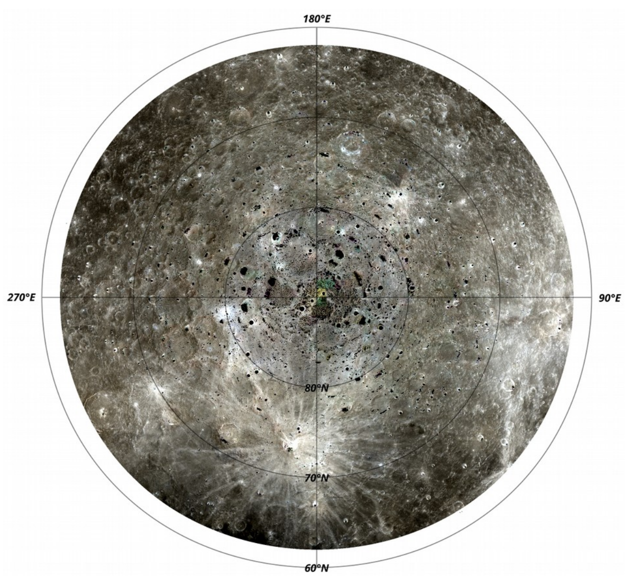

Figure 2. North-polar color composite map (R:689 nm, G:566 nm, B:415 nm; >62°N) in the Cassini projection.

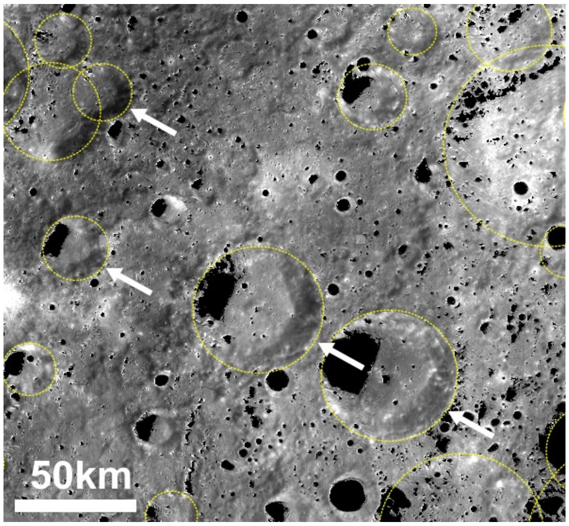

Figure 3. North polar median mosaic in 689 nm band in the Cassini projection. Image center is 80.2°N, 243.5°E. The north pole is toward the lower right. Yellow circles indicate the craters with >20 km in diameter. Arrows point the equator-facing crater walls with the reduced reflectance. Dark areas are the permanent shadow regions.

and several unnamed craters) relative to the surrounding highlands. In the longitudes ranging from 220°E to 260°E (front-farside) and from 40°W to 40°E (nearside), the ***w*** decreases toward the equator in all the wavelengths (e.g., from ~0.4 to ~0.3 in 643 nm band). The lower ***w*** in the nearside is the vicinity of Mare Frigoris, possibly contaminated with the mare ejecta. The farside low ***w*** area is in the middle of highland, free from mare ejecta or regional low reflectance materials. No plausible explanation was found for the origin of this low ***w*** area.

The polar median mosaic (Fig. 2) has almost no shadows (except the permanent shadow regions) and minimum topographic reliefs, meaning that the angle calculations (***i***, ***e***, and ***g***) were accurate enough. There is a minor color shift above 80°N (<2.2 % bluer; higher in 415 nm band), possibly related to the systematically fewer observations (43% on average relative to the latitudes <80°N) in this area which can cause a different fraction of pixel scales. The equator-facing slopes (e.g., crater walls) often show relatively lower reflectance (Fig. 3, pointed by arrows), particularly in the longitudes from 220°E to 260°E where the ***w*** decreases toward the equator (Fig. 1). The reflectance on the flat surfaces (slope < 1°) also gradually decreases from the high latitudes (~80°N) to the mid-latitudes (~65°N) in all the wavelengths (Fig. 4). We note that the areas of major high-reflectance ejecta deposits (e.g., from Anaxagoras, Catena Sylvester, Rozhdestvenskiy K) and the vicinities of Mare Frigoris were excluded from the computation of this trend. Both the lower latitudes and the equator-facing slopes correspond to the areas with lower angles of ***i***.

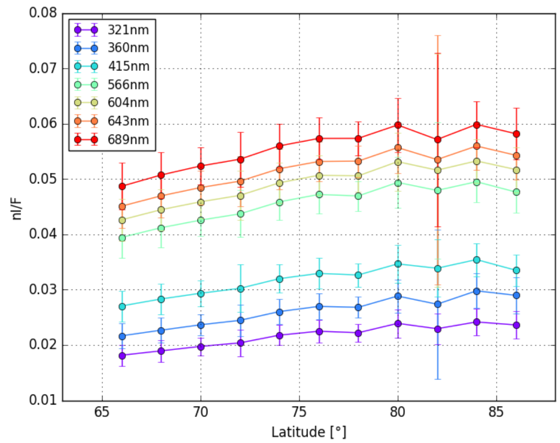

Figure 4. Latitudinal trend of normalized I/F for the flat surface with the slope angle <1°. Dots and error bars indicate the median and standard deviation in each bin (2° in latitude and whole longitude), respectively.

There are several possible origins of this decreased reflectance with the ***i***. The increased residuals of the photometric normalization in high ***i*** angles may cause the increased reflectance (thus relatively decreased with lower ***i***). However, it is unlikely in our tile-by-tile method. Since the fit is optimized for the given range of ***i*** within each tile, no cumulative residuals with latitudes can occur. Actually, this latitudinal trend was not found on the steep slopes (>20°) where the more frequent resurfacing by slope failures are expected. The photometric artifacts can occur on any slope angles, which is not the case here.

If the actual albedo was locally reduced as a function of ***i***, the different intensities of the space weathering might be the possible origin (rather than the compositional variation) as suggested by the 1 μm active measurements by LOLA [3]. Theoretical estimates of the space weathering intensities as a function of ***i*** will allow more accurate comparisons with the observed reflectance drop in our WAC polar color mosaic, which will constrain the mechanisms of the space weathering.

References: [1] Sato et al. (2014a) *LPSC XLV*, Abstract #2281. [2] Heimingway et al. (2015) *Icarus*, 261, 66-79. [3] Lemelin et al. (2016) *Icarus*, 273, 315-328. [4] Sato et al. (2014b) *JGR-Planets*, 119, 1775-1805. [5] Hapke (2012) *Cambridge Univ. Press*, NY. [6] Robinson et al. (2010) *Space Sci. Rev.* 150, 81–124. [7] Sato et al. (2017) *LPSC XLVIII*, Abstract #1139. [8] Haruyama et al. (2012) *LPSC XLIII*, Abstract #1200. [9] Smith, et al. (2011) *LPSC XLII*, Abstract #2350.